ISSN (Print) 1226-1750
ISSN (Online) 2233-6656
Journal of Magnetics 23(1), 1-4 (2018) https://doi.org/10.4283/JMAG.2018.23.1.001

Magnetic and Electrical Properties of Spinel Copper Ferrite Thin Films

Kwang Joo Kim[1], Jongho Park[1], and Jae Yun Park[2,3]*

[1]*Department of Physics, Konkuk University, Seoul 05029, Republic of Korea*
[2]*Department of Materials Science and Engineering, Incheon National University, Incheon 22012, Republic of Korea*
[3]*Research Institute for Engineering and Technology, Incheon National University, Incheon 22012, Republic of Korea*

(Received 21 October 2017, Received in final form 17 January 2018, Accepted 19 January 2018)

Copper ferrite ($Cu_xFe_{3-x}O_4$) thin films synthesized on α-Al_2O_3(0001) substrates exhibited the spinel structure for Cu compositions up to x = 1.0. The substituent Cu ions exhibited charge valence of +2, occupying both the tetrahedral and the octahedral sites of the spinel lattice. Magnetic hysteresis measurements on the $Cu_xFe_{3-x}O_4$ films revealed gradual loss of saturation magnetization (M_s) with increasing x: M_s is reduced to ~50 % that of Fe_3O_4 for x = 1.0. The electrical resistivity (ρ) of the $Cu_xFe_{3-x}O_4$ films increased with x: ρ for x = 1.0 is larger by a factor of 30 than that of Fe_3O_4. The evolution of the magnetic and electrical properties of $Cu_xFe_{3-x}O_4$ can be explained in terms of the competition between the tetrahedral and octahedral Cu^{2+} density for ferrimagnetic moment and polaronic conduction.

Keywords : copper ferrite, sol-gel, ferrite thin film, magnetization, electrical resistivity

1. Introduction

Ferrimagnetic oxide compounds have been drawing a wide range of research interest for their remarkable magnetic and electronic properties for diverse potential applications including information storage, magnetic sensing, microwave absorption, and biomedicine [1-4]. Recently, ferrimagnetic oxides with chemical and thermal stability were reported to be viable anodes for lithium rechargeable batteries [5, 6].

In the spinel lattice of ferrimagnetic oxides, magnetic ions such as Fe^{2+} and Fe^{3+} are distributed over crystallographically distinct tetrahedral 8*a* (A) and octahedral 16*d* (B) sites surrounded by relatively larger O^{2-} ions at 32*e* sites. As the oldest ferrite known to mankind, magnetite (Fe_3O_4) has the inverse-spinel structure in which the A sites are occupied by Fe^{3+} ions, whereas the B sites are equally populated by $Fe^{3+}(d^5)$ and $Fe^{2+}(d^6)$ ions. The angle A-O-B is closer to 180° than those of B-O-B and A-O-A, thus, the Fe^{3+}(A)-Fe^{2+}(B) pair is under a super-exchange interaction (J_{AB}) with anti-parallel spins, while the Fe^{3+}(B)-Fe^{2+}(B) pair is under a double-exchange interaction (J_{BB}) with parallel spins [7]. The ferrimagnetism becomes prominent when J_{AB} is stronger than J_{BB}. Inverse spinel Fe_3O_4 is also known as a good electrical conductor with the conductivity increasing with increasing temperature [8]. There have been reports wherein the electrical conduction in Fe_3O_4 could be understood in terms of polaronic electron hopping between Fe^{2+}(B) and Fe^{3+}(B) sites [9, 10].

When a number of Cu ions substitute the cationic sublattice of Fe_3O_4, the resultant $Cu_xFe_{3-x}O_4$ is likely to have electronic and magnetic properties evolved from those of Fe_3O_4. The charge valence and preferred cationic site of the substituent Cu ions are considered as mainly affecting the site distribution and density of Fe^{2+} and Fe^{3+} ions, leading to a variation in the physical properties of $Cu_xFe_{3-x}O_4$ from those of magnetite.

In this work, thin-film $Cu_xFe_{3-x}O_4$ with phase purity were synthesized using a sol-gel technique up to x = 1.0. The structural, magnetic, and electrical properties of the $Cu_xFe_{3-x}O_4$ thin films were investigated by X-ray diffraction (XRD), X-ray photoelectron spectroscopy (XPS), vibrating sample magnetometry (VSM), and Hall-effect measurements in comparison with those of Fe_3O_4. Although there have been a number of works on magnetic properties of stoichiometric $CuFe_2O_4$ [11, 12], solid solution $Cu_xFe_{3-x}O_4$ system has not been examined to the same extent. The sol-gel method is known to be efficient for synthesizing transition-metal oxide films in uniformity of

*Corresponding author: Tel: +82-32-835-8271
Fax: +82-32-835-0778, e-mail: pjy@inu.ac.kr

grains, deposition rate, and compositional variation. With flat surface, the film specimens are also efficient for investigating electrical properties of the $Cu_xFe_{3-x}O_4$ system. The role of Cu for the magnetic and electrical properties of the Fe-based ferrite was discussed on the basis of the observed experimental data.

2. Experimental

The $Cu_xFe_{3-x}O_4$ specimens were prepared as thin films by using a sol-gel method that is able to provide precursors homogeneous to molecular level. The precursor solution was prepared by dissolving $Fe(NO_3)_3{\cdot}9H_2O$ and $Cu(CH_3CO_2)_2{\cdot}H_2O$ powders together in 2-methoxyethanol at room temperature. The substrate, α-Al_2O_3(0001), was spin-coated by the precursor solution at 3000 rpm for 20 s and then heated at 300 ºC for 4 min. The same process was repeated for increasing the film thickness. All film specimens were obtained through post-annealing in evacuated (~10^{-3} Torr) quartz tube at 800 ºC for 4 h.

The crystal structure of as-prepared specimens was characterized by XRD with Cu K_α radiation (0.15406 nm) in the grazing-incidence manner with fixed X-ray incidence angle of 4º. The surface chemical states about Cu of $Cu_xFe_{3-x}O_4$ films were investigated by XPS with Al K_α radiation (1486.6 eV). The magnetic hysteresis curves of the $Cu_xFe_{3-x}O_4$ films were measured by using VSM at room temperature with magnetic field H ($\leq$ 10 kOe) applied parallel to square-shaped film plane.

3. Results and Discussion

In Fig. 1, the XRD plots of the $Cu_xFe_{3-x}O_4$ ($x \leq 1.0$) films prepared by the sol-gel process are exhibited. The observed XRD peaks indicate spinel-phased polycrystalline $Cu_xFe_{3-x}O_4$ and exhibit little shift of the 2θ from those of the magnetite specimen. It implies little change in the lattice parameter of Fe_3O_4 by Cu doping that is attributable to poor physical contrast of XRD between Cu and Fe. The lattice parameter of each specimen was calculated by extrapolating the values obtained from individual XRD peak positions and the corresponding Miller indices by using the Nelson-Riley function. As listed in Table 1, the lattice parameters of the $Cu_xFe_{3-x}O_4$ specimens are between 0.8371 nm (x = 0.0) and 0.8339 nm (x = 1.0), close to those in literature, 0.8385 nm (JCPDS 88-0866) and 0.8349 nm (JCPDS 25-0283), respectively. The XRD patterns also disclose neither a phase decomposition observed in $Co_xFe_{3-x}O_4$ [13] nor a tetragonal distortion observed in $Ni_xFe_{3-x}O_4$ [14]. However, the XRD data disclosed two small peaks: one near 33.2º for x = 0.2 and the other near 50.5º for x = 0.8 and 1.0 as denoted by α and β in Fig. 1. The peak α is identified as the (104) diffraction of rhombohedral Fe_2O_3 (JCPDS 87-1166), while the peak β is identified as the (200) diffraction of fcc Cu (JCPDS 85-1326).

Table 1. Lattice parameters of polycrystalline $Cu_xFe_{3-x}O_4$ films.

Cu composition (x)	Lattice parameter (nm)
0.0	0.8371
0.2	0.8354
0.4	0.8345
0.6	0.8351
0.8	0.8356
1.0	0.8339

The Cu 2*p*-electron binding-energy (BE) spectra of the $Cu_xFe_{3-x}O_4$ specimens obtained by the XPS measurements are exhibited in Fig. 2. The Cu 2*p* spectra consist of spin-orbit-split $2p_{3/2}$ and $2p_{1/2}$ peaks and satellites which are known to be sensitive to the charge valence of Cu ions in spinel $Cu_xFe_{3-x}O_4$. Both Cu $2p_{3/2}$ and $2p_{1/2}$ peaks consist

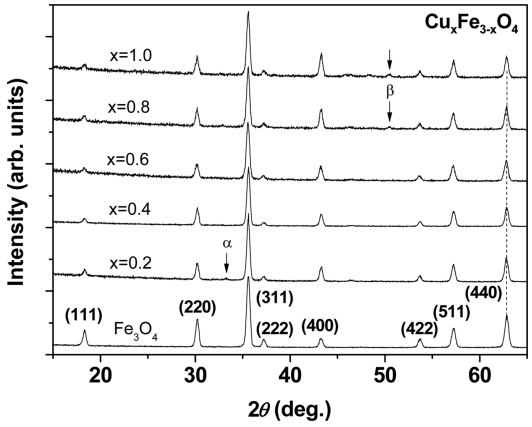

Fig. 1. X-ray diffraction plots of polycrystalline $Cu_xFe_{3-x}O_4$ films.

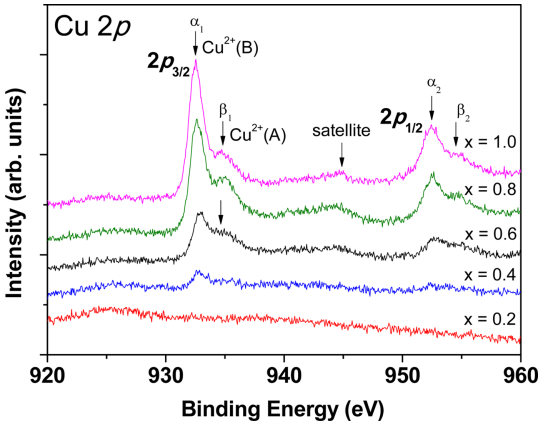

Fig. 2. (Color online) X-ray photoelectron spectra of Cu 2*p* electrons in $Cu_xFe_{3-x}O_4$ films.

of two lines and gain strength gradually with increasing Cu composition. The lines α_1 and α_2, corresponding to Cu $2p_{3/2}$ (932.5 eV) and $2p_{1/2}$ (952.4 eV), respectively, as indicated in Fig. 2, are ascribed to Cu^{2+}(B) ions [11]. On the other hand, the lines β_1 and β_2, corresponding to Cu $2p_{3/2}$ (934.7 eV) and $2p_{1/2}$ (954.6 eV), respectively, are ascribed to Cu^{2+}(A) ions [11]. The broad satellite peak near 945 eV has been ascribed to Cu^{2+} ions in copper oxides [15].

The binding energy of a Cu $2p$ electron under a crystal field of eight (octahedral) O^{2-} ions is expected to be smaller than that under the field of four (tetrahedral) O^{2-} ions. The ratio of line intensity [16] between α_1 and β_1 obtained by estimating their curve-fitted areas is 4:1 for the x = 1.0 specimen, implying that ~20 % of the Cu^{2+} ions are located at the tetrahedral sites.

Magnetic hysteresis measurements were performed on the ferrite films at room temperature by using VSM as shown in Fig. 3. The thickness of the magnetic films estimated by using scanning electron microscopy was in the 0.7~0.8 μm range. The $Cu_xFe_{3-x}O_4$ films show magnetization well saturated at the external magnetic field of 10 kOe. The saturation magnetization (M_s) of the $Cu_xFe_{3-x}O_4$ specimen shows a gradual decrease with increasing x from that of pristine Fe_3O_4 specimen, 415 emu/cm^3 (= 83 % of the theoretical value of 500 emu/cm^3 corresponding to net spin magnetic moment of 4 μ_B per formula unit). For the x = 1.0 ($CuFe_2O_4$) specimen, M_s is observed to be 212 emu/cm^3, being 51 % of the observed value for the Fe_3O_4 specimen. The observed M_s of the $CuFe_2O_4$ specimen is about 77 % of a theoretical value of 275 emu/cm^3 (= 2.2 μ_B per formula unit), estimated for a mixed spinel $(Cu^{2+}_{0.15}Fe^{3+}_{0.85})_{tet}[Cu^{2+}_{0.85}Fe^{3+}_{1.15}]_{oct}O_4$ [11]. The ratio between the observed and the theoretical M_s for the $CuFe_2O_4$ specimen is seen to be close to the corresponding value for the Fe_3O_4 specimen.

In Fig. 4, the variation of M_s with x is displayed as open circles. Also, a dashed straight line is drawn between 415 (at x = 0) and 100 emu/cm^3 (at x = 1.0). In case that all Cu^{2+}(d^9) ions occupy the octahedral sites, the net spin magnetic moment for x = 1.0 ($CuFe_2O_4$) would be 1 μ_B per formula unit when the ferrimagnetic order prevails. So, the expected value of M_s for $CuFe_2O_4$ with octahedral Cu^{2+} is ~25 % (~100 emu/cm^3) of that of Fe_3O_4. It is seen that the value of M_s deviates significantly from the straight line for x > 0.4. The deviation can be understood in terms of the appearance of tetrahedral Cu^{2+} ions for the Cu composition above x = 0.4. The net magnetic moment from the tetrahedral sites is expected to be reduced due to smaller magnetic moment of the Cu^{2+} (1 μ_B) ion than that of Fe^{3+} (5 μ_B) ion. Such reduction in the tetrahedral magnetic moment led to an increase in the net magnetic moment of the spinel $Cu_xFe_{3-x}O_4$ under the ferrimagnetic order.

The DC electrical resistivities of the ferrite specimens were measured using a van der Pauw method under an external magnetic field of 10 kOe at room temperature. As shown in Fig. 5, the electrical resistivity (ρ) of the $Cu_xFe_{3-x}O_4$ film increases with increasing Cu composition from 5.5 × 10^{-2} Ω·cm for x = 0 (Fe_3O_4) to 1.7 Ω·cm for x = 1.0 (increase by a factor of 30). The good electrical conductivity of Fe_3O_4 can be understood based on thermally activated electron hopping between octahedral Fe^{2+}(d^6) and Fe^{3+}(d^5) sites [9]. The minimum distance between the octahedral cations is ~0.3 nm, estimated from the lattice parameter of Fe_3O_4 (0.8385 nm). The electron hopping in the cationic sublattice has been theoretically formulated in terms of transport of small polaron, composed of an electron and surrounding acoustic phonons [17, 18]. Such

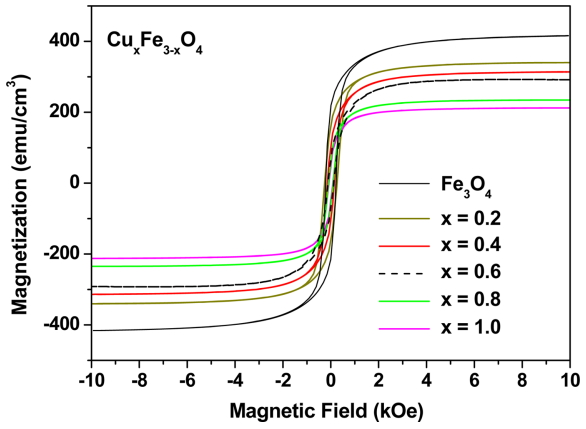

Fig. 3. (Color online) Magnetic hysteresis curves of $Cu_xFe_{3-x}O_4$ films measured by vibrating sample magnetometry at room temperature with external magnetic field parallel to the film plane.

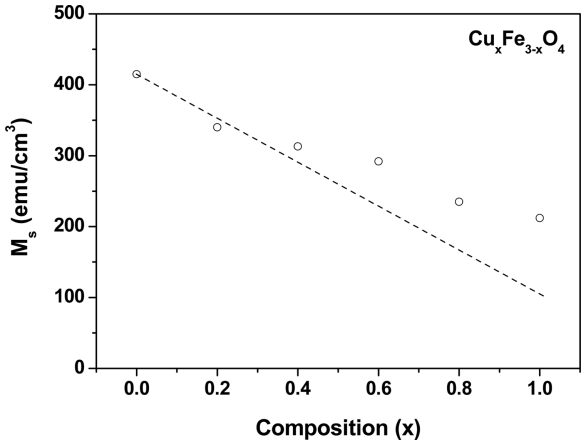

Fig. 4. Saturation magnetization at H = 10 kOe of $Cu_xFe_{3-x}O_4$ films obtained from the respective magnetic hysteresis curves.

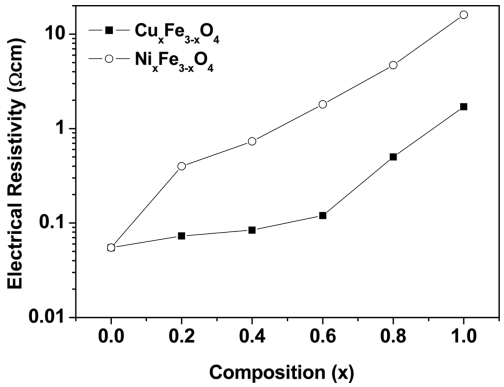

Fig. 5. Electrical resistivities of $Cu_xFe_{3-x}O_4$ films. Electrical resistivities of $Ni_xFe_{3-x}O_4$ films are exhibited for comparison with those of $Cu_xFe_{3-x}O_4$.

polaronic conductivity is likely to be sensitive to the cation distribution in the crystal lattice. Thus, the increase in ρ with increasing x for $Cu_xFe_{3-x}O_4$ is ascribed primarily to the decrease in octahedral Fe^{2+} population caused by the Cu^{2+} substitution, resulting in a decrease in octahedral Fe^{2+}-Fe^{3+} polaronic hopping rate.

The variation of ρ for $Cu_xFe_{3-x}O_4$ is compared with that of $Ni_xFe_{3-x}O_4$ in Fig. 5. The $Ni_xFe_{3-x}O_4$ films for the Hall measurements were prepared following the sol-gel process described in ref. 19. It is seen that the value of ρ for $Ni_xFe_{3-x}O_4$ increases with x faster than that for $Cu_xFe_{3-x}O_4$: at x = 1.0, ρ = 16 Ω·cm for $Ni_xFe_{3-x}O_4$, being larger by a factor of ~10 than that for $Cu_xFe_{3-x}O_4$. The ionic valence of Ni in the $Ni_xFe_{3-x}O_4$ specimens was found to be +2 [19], same as that of Cu in the present $Cu_xFe_{3-x}O_4$ specimens. Thus, the difference in ρ between the two compounds is primarily attributable to significant tetrahedral Cu^{2+} density in $Cu_xFe_{3-x}O_4$, while the Ni^{2+} ions in $Ni_xFe_{3-x}O_4$ exist mostly in the octahedral sites [19, 20].

4. Conclusions

The spinel $Cu_xFe_{3-x}O_4$ ($x \leq 1.0$) thin films have been successfully deposited on α-Al_2O_3(0001) substrates by using a sol-gel process. X-ray diffraction data indicated that Fe and Cu mix properly to solid-solution $Cu_xFe_{3-x}O_4$ without lattice deformation. The Cu ions in the $Cu_xFe_{3-x}O_4$ specimens exist as Cu^{2+} at tetrahedral as well as octahedral sites. The magnetic hysteresis curves of $Cu_xFe_{3-x}O_4$ are well saturated under the external field of 10 kOe and exhibit decreasing M_s with increasing Cu composition. The decreasing trend of M_s can be understood in terms of the majority and minority of Cu^{2+} ions at octahedral and tetrahedral sites, respectively. The increase in electrical resistivity of $Cu_xFe_{3-x}O_4$ with increasing x is understood as due to a decrease in polaronic hopping rate of electron between octahedral Fe^{2+} and Fe^{3+} ions.

Acknowledgments

This work was supported by Incheon National University Research Grant in 2016.

References

[1] J. A. Paulsen, A. P. Ring, C. C. H. Lo, J. E. Snyder, and D. C. Jiles, J. Appl. Phys. **97**, 044502 (2005).
[2] C. W. Nan, M. I. Bichurin, D. Shuxiang, D. Viehland, and G. Srinivasan, J. Appl. Phys. **103**, 031101 (2008).
[3] X. Gu, W. Zhu, C. Zia, R. Zhao, and W. Schmidt, Chem. Commun. **47**, 5337 (2011).
[4] J. Singh, A. Roychoudhury, M. Srivastava, V. Chaudhary, R. Prasanna, D. W. Lee, S. H. Lee, and B. D. Malhotra, J. Phys. Chem. **117**, 8491 (2013).
[5] X. Liu, T. Zhang, Y. Qu, G. Tian, H. Yue, D. Zhang, and S. Feng, Electrochim. Acta **231**, 27 (2017).
[6] Y. Zhao, X. Zhai, D. Yan, C. Ding, N. Wu, D. Su, Y. Zhao, H. Zhou, X. Zhao, J. Li, and H. Jin, Electrochim. Acta **243**, 18 (2017).
[7] D. Tripathy, A. O. Adeyeye, C. B. Boothroyd, and S. N. Piramanayagam, J. Appl. Phys. **101**, 013904 (2007).
[8] S. B. Ogale, K. Ghosh, R. P. Sharma, R. L. Greene, R. Ramesh, and T. Venkatesan, Phys. Rev. B **57**, 7823 (1998).
[9] C.-H. Lai, P.-H. Huang, Y.-J. Wang, and R. T. Huang, J. Appl. Phys. **95**, 7222 (2004).
[10] R. Gupta, A. K. Sood, P. Metcalf, and J. M. Honig, Phys. Rev. B **65**, 104430 (2002).
[11] C. Reitz, C. Suchomski, J. Haetge, T. Leichtweiss, Z. Jaglicic, I. Djerdj, and T. Brezesinski, Chem. Commun. **48**, 4471 (2012).
[12] D. Gingasu, I. Mindru, L. Patron, and C.-B. Cizmas, J. Alloys Compd. **460**, 627 (2008).
[13] K. J. Kim, J. H. Lee, and C. S. Kim, J. Korean Phys. Soc. **61**, 1274 (2012).
[14] K. J. Kim, M. H. Kim, and C. S. Kim, J. Magn. **19**, 111 (2014).
[15] J. Kwon, J. M. Ducere, P. Alphonse, M. Bahrami, M. Petrantoni, J.-F. Veyan, C. Tenailleau, A. Esteve, C. Rossi, and Y. J. Chabal, Appl. Mater. Interfaces **5**, 605 (2013).
[16] K. J. Kim and T. Y. Koh, J. Sol-Gel Sci. Technol. **77**, 528 (2016).
[17] R. Schmidt, A. Basu, and A. W. Brinkman, Phys. Rev. B **72**, 115101 (2005).
[18] A. Karmakar, S. Majumdar, and S. Giri, Phys. Rev. B **79**, 094406 (2009).
[19] K. J. Kim, T. Y. Koh, J. Park, and J. Y. Park, J. Magn. **22**, 360 (2017).
[20] A. Ahlawat, V. G. Sathe, V. R. Reddy, and A. Gupta, J. Magn. Magn. Mater. **323**, 2049 (2011).